Extent of Submarine Volcanic Plume Deposition Offshore Olosega Island in American Samoa

Sophie Goddard

University of Washington, Seattle, WA

School of Oceanography, Box 357940

Seattle WA 98195-7940

sgoddard@uw.edu

3/8/2024

Abstract

There has been little mapping of the seafloor, resulting in a large lack of knowledge of seafloor environments. It is important to map the seafloor for numerous reasons, such as being able to predict and mitigate public risk from tsunamis caused by faulting, determining what habitat locations are best to anchor alternative energy infrastructure, and monitoring the health of organisms and their habitats on the seafloor. In order to get a better understanding of the impact of volcanic submarine sediment on seafloor environments, we mapped and collected sediments at an 1866 eruption site between the Manu'a Islands in American Samoa. The goal of this research is to get a first look at the post-eruption bathymetry, evaluate where the volcanic sediment settled, determine the size and type of the volcanic sediment, and assess how the bathymetry of the seafloor changed from the eruption. This data was collected on a 14-day cruise on the R/V Thompson in American Samoa and used a multibeam sonar system to map the seafloor bathymetry and a grab sampler to take sediment samples. Eight volcanic sediment samples were collected and processed. These comprised of sand and gravel sized (400-4300 μm) fragments of volcanic origination. We were not able to say that the grain size data showed a strong correlation with distance from the eruption site and backscatter, as we only could process seven sediment samples and were unable to date them to the eruption. We were able to map the eruption site and the surrounding seabed, finding evidence of other geological processes such as landslides and more volcanoes. This data gives us greater insight into the settling processes after an eruption and helps us predict future effects and impacts from submarine eruptions.

Plain Language Summary

Studying the seafloor is fundamental in helping us understand the complex environments in the ocean. The seafloor can affect the chemistry of seawater, water and heat circulation, and many other critical processes. One way to study the seafloor is through using sensors and making

bathymetric maps, like topographic maps on land. This paper will look at a specific volcanic eruption in American Samoa to see how the eruption process affected the seafloor, which can help us predict future changes from eruptions. This data was collected on a 14-day cruise on the R/V Thompson in American Samoa. To study this eruption site, we used a grab sampler that we dropped from the ship down to the seafloor. Once it hits the seafloor, a spring releases and grabs a handful of sediments. From this, I can study the sediments from different locations around the eruption site to see the characteristics of the volcanic sedimentation. Back in the lab, the samples were put into a machine to be separated by size. Once broken up, we could measure individual grain sizes. The sediments ranged from fine sand to coarse gravel and were poorly sorted, meaning there was a large variation in the sizes of the grains. The range in average grain size at each location was 400-4300 μm. There was a weak trend in average grain size increasing when approaching the eruption site. To map the bathymetry, the seafloor depth, we used a sensor that uses the time a sound wave takes to hit the seafloor and come back up to the ship. From this data we can make bathymetric maps of the seafloor. This mapping data will also fill in missing areas on global databases, where mapping data from scientific boats across the world are compiled to make comprehensive seafloor bathymetric maps.

Introduction

Marine volcanic eruptions are critical to study as they can impact water temperature, sea height levels, oxygen concentrations, carbon cycling, and change the seabed and benthic habitats existing on the flanks of submarine volcanoes. Eruptions start when plumes of hot mantle material rise from the lower mantle. As the plumes rise to the upper mantle, they undergo partial melting and upwell to the surface, creating the formation of submarine volcanoes and hotspot environments. (Rubin et al. 2012). These hotspot environments can be found at convergent or divergent plate boundaries (Cañón-Tapia et al. 2004). In American Samoa, the Pacific Plate and Australian Plate are converging. The Pacific Plate is subducting under the Australian Plate. A chain of hotspot volcanoes commonly forms on these plate boundaries, such as in American Samoa, and are prone to earthquakes (Jackson et al. 2017). In 1866 there was a volcanic eruption at the island Olosega (American Samoa) creating a caldera, a crater-like structure, from the explosion. These islands in American Samoa are on a hotspot chain where volcanic activity is regular. The eruption at Olosega has had no extensive mapping, but we do have mapping and research from other volcanic hotspots and eruptions, such as in Hawaii (Morgan et al. 2003). In current global bathymetric maps, there is a lack of data around

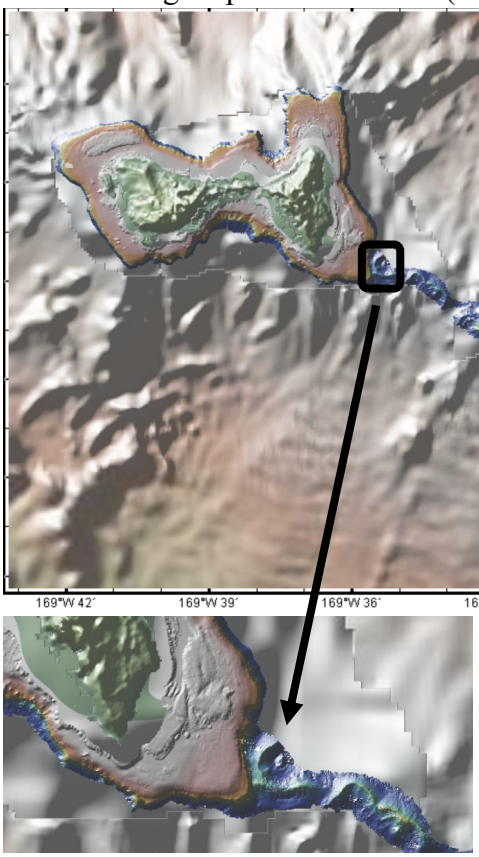

Figure 1. Map of American Samoa islands, Olosega and Ta'ū, with the caldera from the 1866 eruption boxed in black. The map below is a zoomed in area of the caldera, which was missing bathymetry data on the northern side (www.geomapapp.org; Ryan et al. 2009).

the 1866 eruption's site, which means there is insufficient General Bathymetric Chart of the Ocean, GEBCO, data of the surrounding flanks of the eruption site (Fig. 1). GEBCO is an international organization that works to develop and integrate bathymetric datasets. Their aim is to create and make available extensive datasets and maps showing the seafloor shape. GeoMapApp is a map-based application to visualize geoscience datasets, such as GEBCO. Since GeoMapApp holds much of the publicly available mapping data in their bathymetry archive, we know that there has not been extensive mapping in the region of American Samoa, and only the southern half of the caldera has been mapped (Fig. 1).

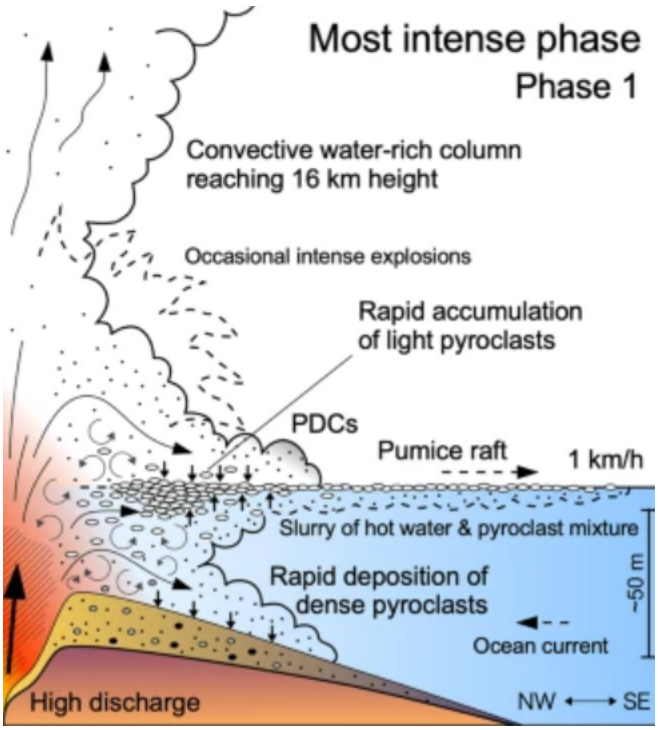

Figure 2. Diagram of the phreatomagmatic explosion at Fukutoku-Oka-no-Ba eruption by the Bonin Islands of Japan in 2021 (Maeno et al.2022).

Literature on types of marine volcanoes and volcanic sediment exists, but not extensively in this Equatorial Pacific region (Houghton et al. 2015). This 1866 eruption was a phreatomagmatic eruption, which means water and magma mixed to make the explosive eruption. Phreatomagmatic eruptions differ from other types as they have juvenile clasts, a fragment of a rock or mineral, and are characterized as explosive eruptions with large amounts of volcanic ash (Fig. 2). The volcanic sediments of these eruptions generally include volcanic ash and finer grain sizes. Previous literature of phreatomagmatic eruptions concluded that volcanic sediments from phreatomagmatic eruptions have less variation in sediment sizes and are better

sorted than other types of eruptions. Based on a study of volcanic grain size at a submarine eruption in Montserrat in the West Indies, the grain size of volcanic sediments ranged around 160-400 µm (Rehm et al. 2003 and Cassidy et al. 2014).

In order to see where the volcanic sediments settle after an eruption, we looked at the seafloor. Acoustic instruments were used to map the seafloor, one of which was a multibeam sonar. The multibeam, which is attached to the bottom of the research vessel, sent a signal or pulse from the transducer that bounced off the bottom/object and then returned an echo to the transducer. The distance was then calculated using the time elapsed between the signal emission and its reception. Multibeam sonar uses multiple transducers on the bottom of the ship, pointing at different angles to get a big-picture map of the seafloor (Hellequin et al. 2003). The multibeam has been used in previous research, such as in the Hawaiian Islands, to help characterize flank morphology, identify geomorphological features and seafloor environments, discern geomorphic zones and regions of erosion, and determine what processes influence morphological changes (Gardner et al. 2021). The multibeam system also provides acoustic backscatter that responds differently among different sediments, and we can correlate the different backscatter values to grain size values (Fig. 3, Wattson et al. 2017). The objective of this study is to determine the extent and sediment characteristics of the phreatomagmatic eruption in 1866 using multibeam sonar and sediment grab samples. I hypothesized that near the

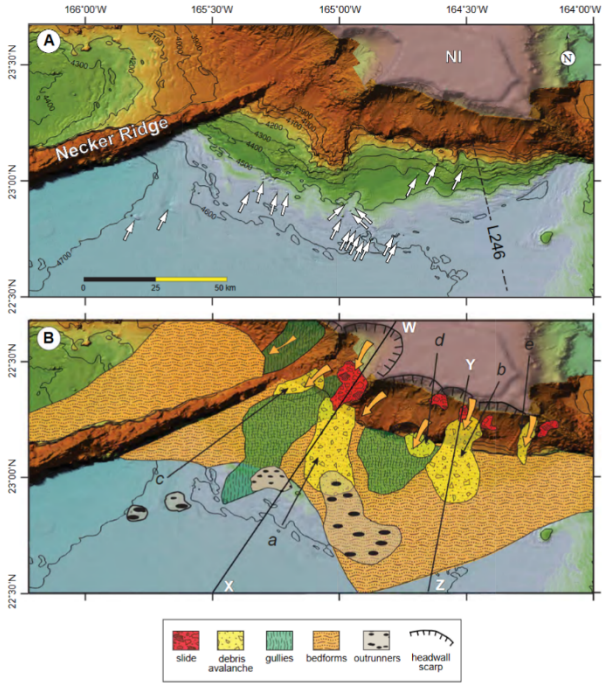

Figure 3. Map of multibeam bathymetry data from bathymetry data in Hawaii, the data was used to determine different sediment types and geological processes (Gardner et al. 2021).

eruption site, there would be higher backscatter values from volcanic sediments, and moving down the flank, away from the eruption site, the texture of the seabed would become less coarse, indicated by smaller grain sizes and concentration of volcanic sedimentation. I predicted that there would be a gradient in grain size, with larger grain sizes being near the caldera and as we moved down the flank, away from the caldera, grain size would decrease.

Methods

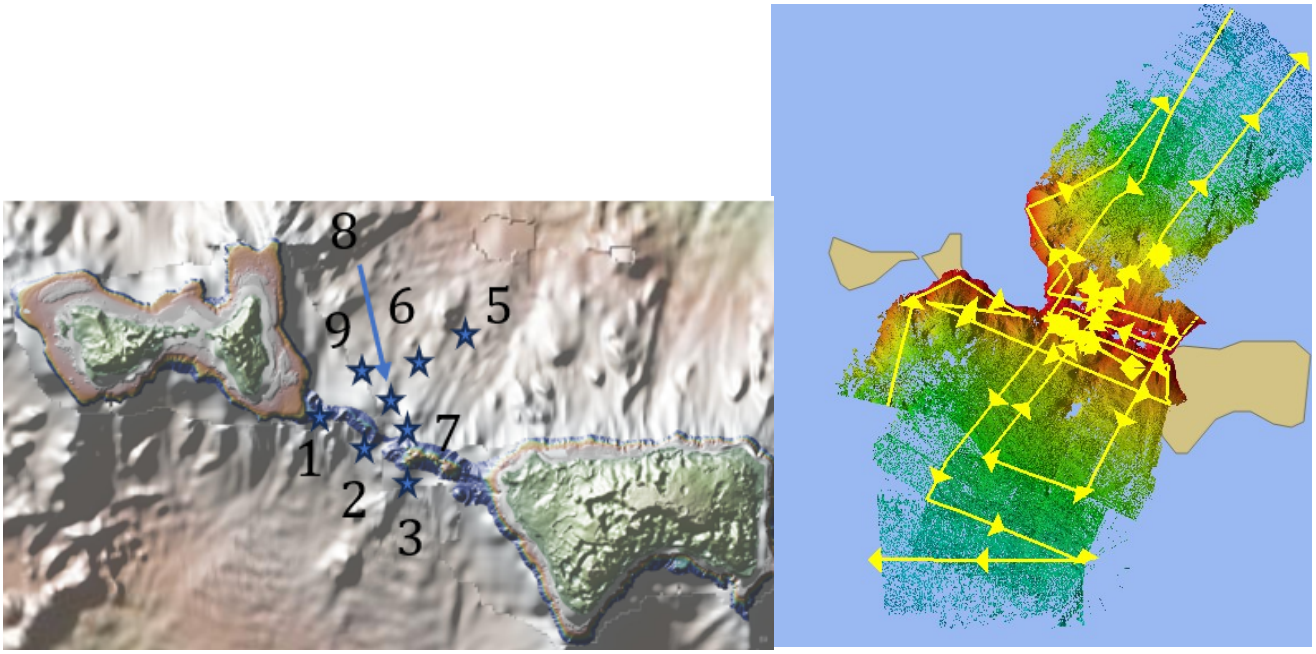

Figure 4. The map on the left, was made by the current bathymetric data in GeoMapApp and has all the grab sample sites marked with green stars. The map on the right is a map created in Qimera with the bathymetry data and the track lines we mapped along in yellow. (www.geomapapp.org; Ryan et al. 2009).

Data was collected on a cruise aboard the R/V Thompson from December 28th, 2023 – January 11th, 2024. We left the port of Pago Pago in American Samoa and then steamed towards the Manu'a islands. We were limited in time as the ship's speed was around six kts to get the quality data we wanted, affecting the time we had to map the bathymetry and how many grab samples we could do. Based on past current data, from ROMS and Earth Model, we determined the NE direction would likely have the most abundant concentration of volcanic sediments. We

determined this by assuming that the currents at the time of the eruption would cause a large number of volcanic sediments to be deposited in the direction of that current. Once in the Manu'a islands, we planned to collect our data for 24 hours, but we had an extra 12 hours of mapping when returning to port and collected three additional grab samples (Fig. 4). The first step in my data collection aboard the ship was using the EM302 multibeam SONAR systems to map the backscatter and roughness of the seafloor at the caldera. We also used the Knudsen 3260 Chirp to see the thin layers of the upper seafloor and the basaltic bottom on the caldera. The last instrument used was the Shipek Grab Sampler to get eight sediment samples as we moved away from the caldera to help calibrate the multibeam data and give us a visual of what type and size of sediment was on the seafloor.

The sediment samples were brought from the ship back to the lab for processing. In the lab, the samples were dried by leaving them in a 60˚ oven overnight. Once dried, we ran them through the RO-TAP, which has a set of sieves that decrease in diameter. The stack of sieves is mechanically shaken to break up the sample and disperse it throughout the sieves. Sediment grains will then be distributed in different sieves based on grain size and weight. The weights per sieve size were then put into the software program Gradistat, which produced averages, sorting distribution, sediment type, and more. Stoke's law was then used to calculate the settling velocity of the particles. In Stokes Law, the diameter of a particle was calculated using the mean grain size, from the Gradistat data, at each site.

$$\boldsymbol{Ws = \frac{D^2 \Delta p g}{18\mu}}$$

Δρ is the density of the particle minus the average density of seawater, g is gravitational acceleration, and μ is the viscosity of seawater at a specific temperature.

The following step was to look at the angularity of the rocks from the grab samples under an AmScope SM-1T Series Zoom Trinocular Stereo Microscope to see how much erosion and weathering had occurred. Smoother rocks have gone through more processes that caused the rock's edges to be eroded. The degree of roundness can help us infer the amount of physical transportation processes the rock has gone through; increased exposure to physical transportation processes causes rocks to be rounder. From this, we can compare the roundness and sphericity of the rocks in the samples to each other to determine relative ages. If they came from the same source, we could determine how the environments they were deposited in differ in weathering processes and if those processes may have disturbed and moved the rocks from where they originally settled (Manual of Sedimentary Petrography, 1988).

A Pearson statistical correlation test was used to calculate the likelihood of correlation between the grain size, backscatter, and distance from the caldera data. This statistical test gave $\mathbf{r^2}$ values that represented the significance and likelihood of the correlation between the data being from chance.

Results

Between December 29th-30th, we mapped between the Manu'a islands using a multibeam to produce bathymetric maps (Fig. 5). We were able to map the rest of the caldera from the 1866 eruption. From this mapping, we know the diameter of the caldera is roughly 750 m, its depth is 300m, and the blow-out is in the NE direction (Fig. 5). The swath of the multibeam was not very wide in the shallow depths, causing some holes in the mapping.

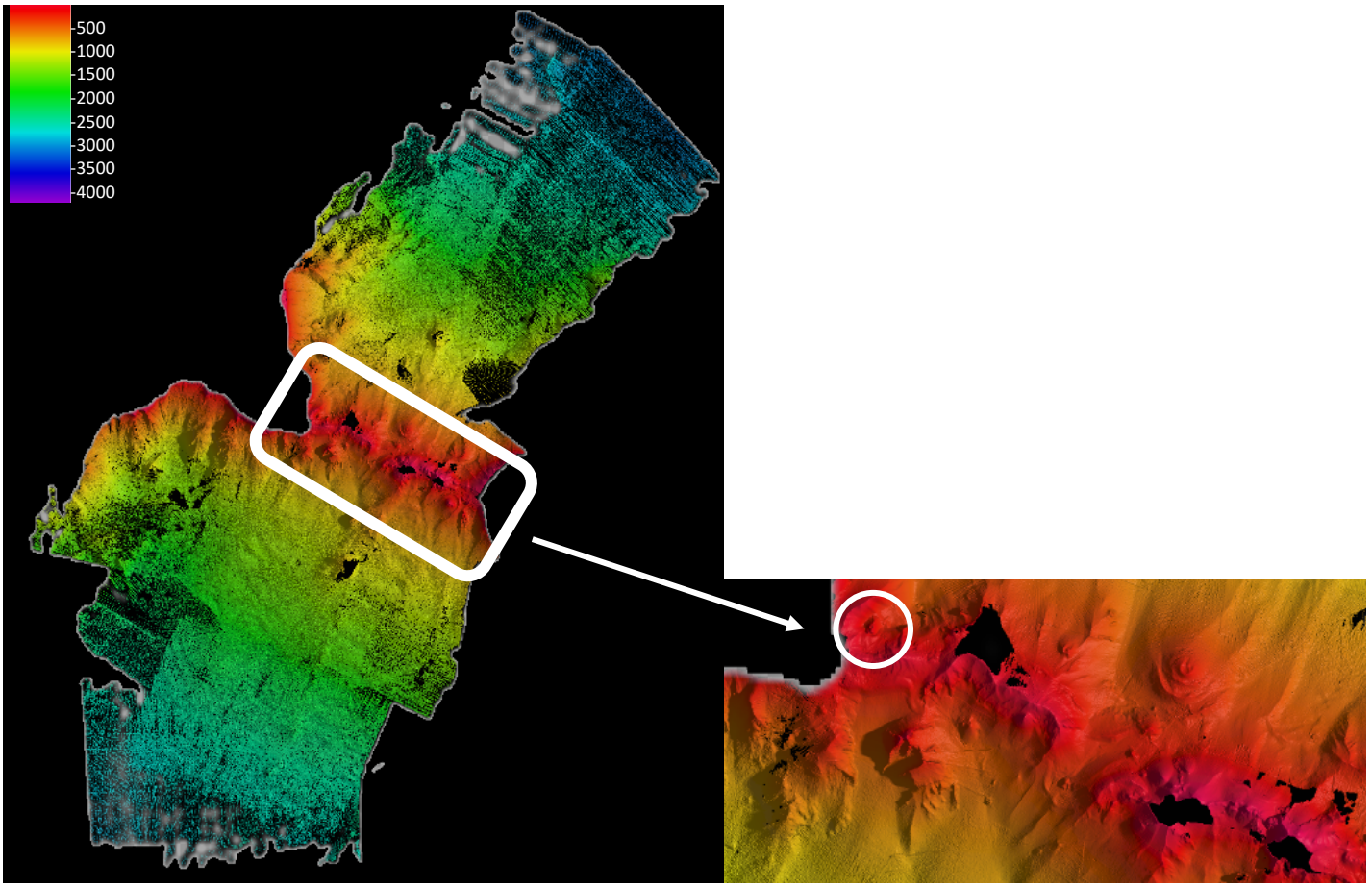

Figure 5. Bathymetry map created using data from the onboard multibeam. The white box encapsulates the shallow area along the ridge, with what looks like to be multiple calderas, including the caldera from the 1866 eruption circled in white.

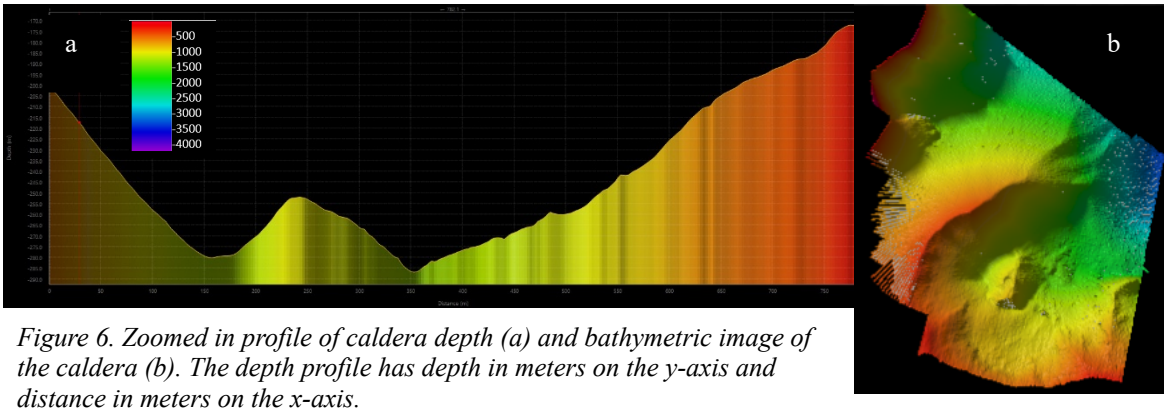

Figure 6. Zoomed in profile of caldera depth (a) and bathymetric image of the caldera (b). The depth profile has depth in meters on the y-axis and distance in meters on the x-axis.

The grab sampler successfully collected volcanic sediments from the seafloor. We were able to take a total of eight grab samples, though, at one of the locations, the grab sample did not have enough sediments to run grain size analysis on. Figure 7 shows the distribution of sediment samples at each sieve size from every location, not just the mean or most abundant. The mean grain size was between 411-4300 µm. All the sample locations were either poorly sorted or very poorly sorted, and the main sediment types were sand and gravel (Table 1).

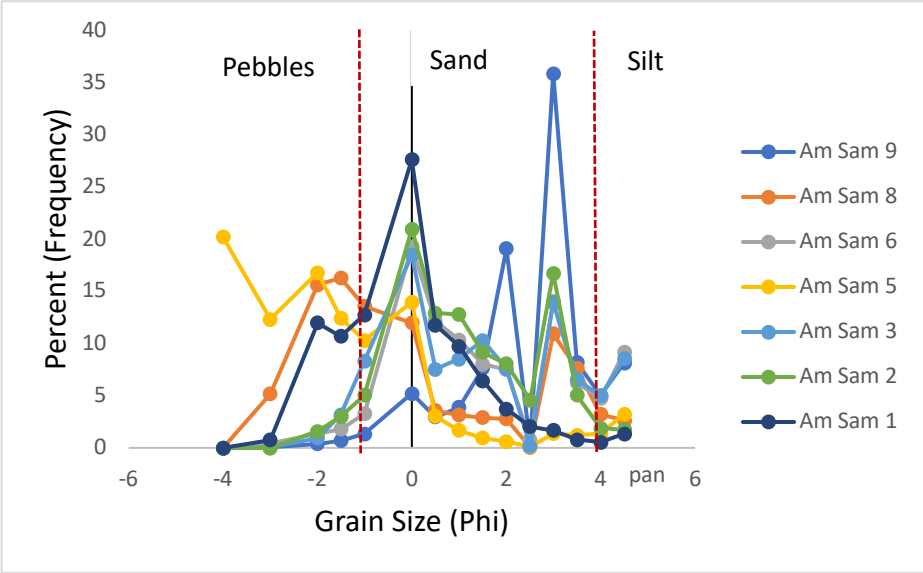

Figure 7. The percent or frequency of a certain grain size at each location. Each sample location is colour coded. The points represent the weight of sediment that was distributed on each sieve on the RO-TAP. The weight at each sieve is associated with a phi value, the size of the sieve net. The percent is the weight of sediment distributed at a certain sieve divided by the total location sediment weight times 100. The red dashed lines indicates where pebbles grains are distributed vs. sand grains.

Table 1. The sediment type, sorting, mean grain size, and settling velocity of the samples at each grab sample.

Sample Name	Sediment Type	Sorting	Mean GS (µm)	Settling Velocity (m/s)
Am Sam 1	Sandy Very Fine Gravel	Poorly Sorted	1342.6	1.48
Am Sam 2	Very Fine Gravelly Coarse Sand	Poorly Sorted	511.5	0.22
Am Sam 3	Very Fine Gravelly Very Coarse Sand	Very Poorly Sorted	434.2	0.16
Am Sam 5	Very Coarse Silty Sandy	Very Poorly Sorted	4248.9	14.8

	Very Fine Gravel			
Am Sam 6	Very Fine Gravelly Coarse Sand	Very Poorly Sorted	411.1	0.14
Am Sam 8	Sandy Very Fine Gravel	Very Poorly Sorted	1113.7	1.02
Am Sam 9	Slightly Very Fine Gravelly Fine Sand	Poorly Sorted	198.8	0.032

There was a slight trend between grain size and distance from the caldera, being that the smaller grain sizes were generally further from the caldera. There was no correlation as the R^2 value was 0.2543. Grab sample 5 was a large outlier and was not included in the statistical analysis tests (Fig. 8).

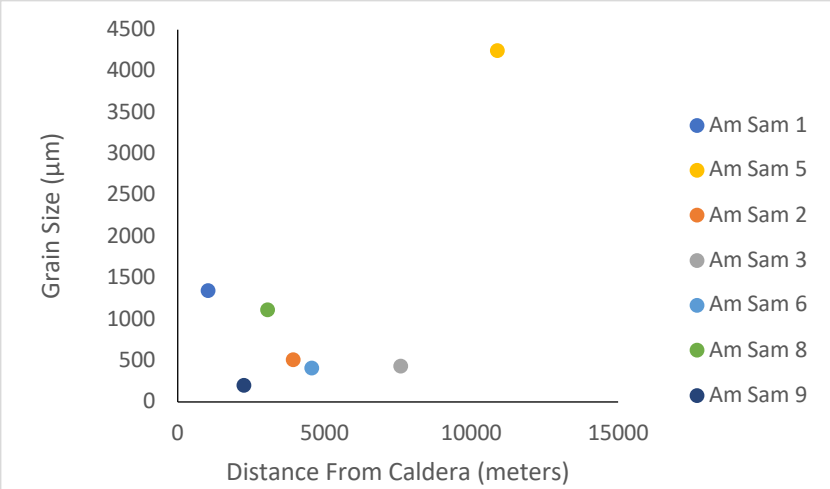

Figure 8. The mean grain size of each sample location on the y-axis plotted against the distance of each grab sample from the caldera on the x-axis.

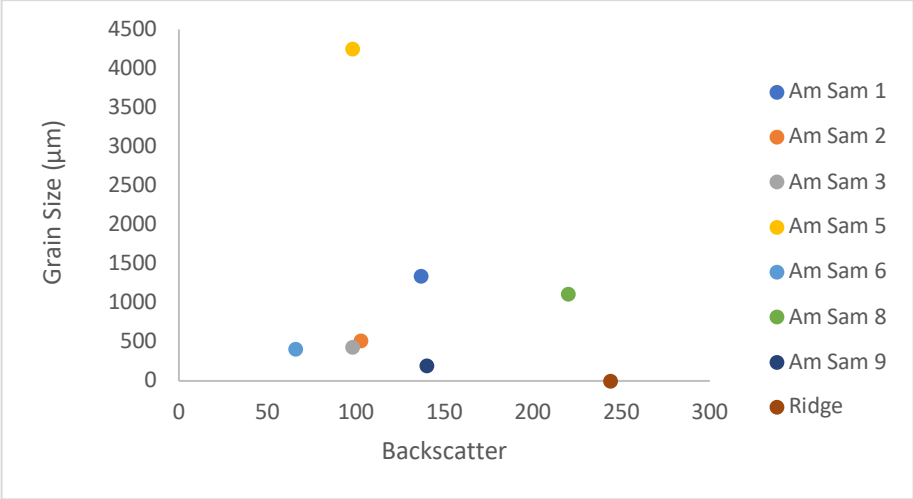

Figure 10. Each grab sample location's mean grain size plotted on the y-axis against the backscatter value at that location on the x-axis.

The backscatter values were mapped in QGIS using the bathymetry data, which was cleaned and processed through Qimera (Fig. 9). There is no statistically significant correlation between

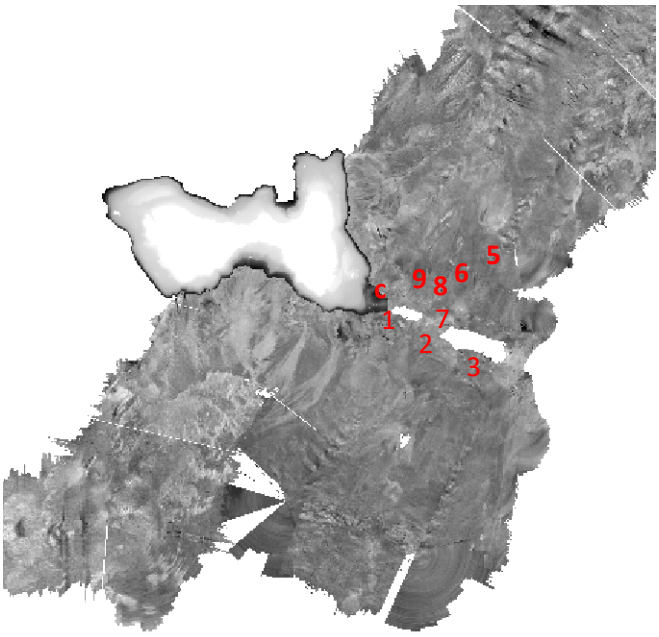

Figure 9. Map of the backscatter from the bathymetry data. The caldera and each grab sample location are labeled in red. The red "c" marks the caldera. Note that location Am Sam 4 was skipped due to time limitations and location Am Sam 7 sample was too small to run grain size analysis on.

grain size and backscatter values. The R^2 value is 0.3257. The caldera and ridgeline had high backscatter values (Fig. 10).

Sphericity and roundness were measured visually via a microscope. Location Am Sam 5 had high sphericity and was sub-rounded, while the rest of the locations were sub-angular to angular and weren't as spherical (Fig. 11). The angularity was highest at Am Sam 5 with an average of 144-152°, while the other three locations had smaller angles ranging between 120-140° (Table 2).

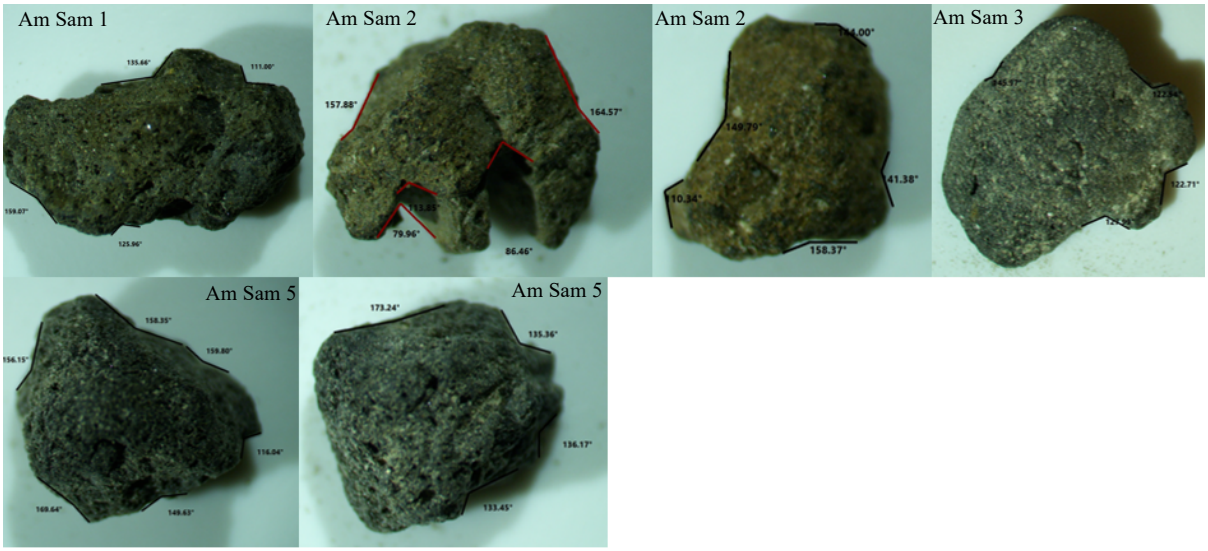

Figure 11. Photos of sediments at three locations grab sample locations on the ridgeline under a microscope. From left to right on the top are samples from locations 3, 3, 2, 7 and on the bottom 1, 5. These photos were used to compare the roundness and sphericity of the sediments.

Table 2. The average angularity of three different grab sample

Location	Average Angularity
Am Sam 1	132.9
Am Sam 2	120.5
Am Sam 2	140.8
Am Sam 3	129.8
Am Sam 5	151.6
Am Sam 5	144.6

Lastly, the average settling velocity was calculated using Stokes' Law and then compared to the predicted velocities on the Wentworth Diagram. The velocities ranged from 3.24E-02-1.48E+01 $^{m}/_{s^2}$ (Table 3).

Table 3. The settling velocity calculated via Stoke's Settling Velocity Law for each grab sample.

Location	Settling Velocity (m s-1)	Depth (m)
Am Sam 1	1.48	450
Am Sam 2	0.22	564
Am Sam 3	0.16	525
Am Sam 5	14.8	1233
Am Sam 6	0.14	803
Am Sam 8	1.02	472
Am Sam 9	0.032	559

Discussion

Due to records of the eruption describing it as explosive, the assumption was made that there would be a gradient in grain size from the eruption on all sides of the caldera. The direction of the current is where we expected to have the best record of sedimentation. From this, I assumed that the direction of the current during the eruption is where there will be a larger gradient in grain size because more of the volcanic sediments were moved in that direction by the advection of the water column from the current. Since I was estimating the direction of the largest gradient of sediment deposition, another direction may have had a better record of the volcanic sediment gradient.

It is difficult to draw conclusive trends with the grain size data because, while mapping, we found a series of calderas along the ridge. The series of calderas on the ridgeline were east of the 1866 eruption site (Fig. 5), as is the newly volcanically active island on this hot spot chain. The diameter of these calderas ranges from 280-900 m with depths from 300-500 m. However, we don't know when they were active, so we can't conclusively say which eruption produced specific deposits. We knew there were likely multiple marine volcanoes and eruption sites as this is a hot spot environment but did not predict that other calderas would be so close, which means that there are multiple plumbing sets for each of these volcanic systems. This finding causes some discrepancy in knowing which caldera the volcanic sediments collected came from. In the future, with more resources, isotopic dating or using trace element analysis could be used to date the sediments to a specific eruption. Isotopic dating would prove hard as the half-lives' of most elements used in isotopic dating are millions of years, and some of these eruptions have occurred in the last couple of hundred years.

The calculated settling velocities were higher than predicted, based on the Wentworth table, because the water was warm and had a low dynamic viscosity. The sample sites near the caldera and on the ridge tended to have the fastest settling velocities, which corresponds to them also having the largest grain sizes. The sites with the slowest settling velocities were further away from the caldera and corresponded to smaller grain sizes. There was no strong correlation between depth and the settling velocity.

I hypothesized that near the eruption site, there would be higher backscatter from volcanic sediments, and moving down the flank, away from the eruption site, the texture of the seabed would become less coarse, indicated by smaller grain sizes and concentration of volcanic sedimentation. There was a slight trend in larger grain sizes being closer to the caldera, loosely

following my prediction. The further the distance away from the caldera, the relationship between distance and grain size seemed to decrease. Our estimation that there would be a large number of volcanic sediments to the northeast of the caldera was correct, which was also the direction of the blowout from the eruption. My overall prediction was not conclusive given the data collected, as there were enough outliers that caused the r^2 value from the statistical analysis tests to be above .05. Statistical analysis tests show the likelihood that the correlation between two variables was by chance rather than the variables being correlated. Statistical analysis tests are not fully conclusive in this situation as the data set was comprised of eight samples, one of which was too small to get any numeric data from.

The relationship between backscatter and grain size is weak at best. The backscatter is high at the caldera and has medium values between sample sites Am Sam 1, 2, 3, 6, and 9 but sites 5 and 8 were outliers, though there was lots of spatial variability. One takeaway was that larger sediments tended to have higher backscatter values, and the backscatter became less representative as we moved farther away from the caldera. As we moved further away, the depth of the water column greatly increased, there were other volcanic sites, and landslides likely occurred.

Sample location Am Sam 5 was an outlier in the grain size and backscatter data. This may be because of other processes, such as landslides, as it is north of the caldera. There is evidence of landslides on the northeast and southeastern sides of the island Olosega, the island on the western side of the caldera. We can tell this by looking at the bathymetry data, where we can see the scarps and smooth bathymetry. It is hard to date these landslides in relativity to the time of the 1866 eruption. There were likely multiple landslides after the 1866 eruption, and if so, they would have disrupted the settled volcanic sediments (Levitan et al. 2024).

The grab sampler at location Am Sam 7 was able to pick up some sediments, but not enough to be analyzed using the RO-TAP to get grain size analysis data. Location Am Sam 7 was on the ridge along the hotspot chain. The sediment at this location stood out because of their distinct colouring compared to the other sample locations. While all the other samples were black and dark grey, basaltic, this sample was brownish orange. The two current explanations are that these rocks are old and covered in manganese, giving the orange colour, or that they are pumice, a volcanic rock with a vesicular texture and comprised of glass.

Angularity suggests that locations closer to the caldera tended to be more angular in shape, except for location Am Sam 7. Locations Am Sam 2, 3, and 7 were on the ridge east of the caldera. Through measuring the degree of roundness via microscope, we can see that Am Sam 5 was more spherical and was sub-rounded. The only other location where the sediments seemed to have high sphericity and be sub-rounded was Am Sam 7, where the unique brown and red colouring can also be seen. This suggests that sediments at site Am Sam 5 went through other processes that weathered its shape and may have disrupted where it settled.

My prediction on grain size distribution relative to the caldera was based on the idea that larger clasts have a faster settling velocities, resulting in them being deposited closer to the caldera than smaller grain-size sediments (Stokes' Law). My findings partially support this, as generally, the larger grain sizes were at locations closer to the caldera. The outliers in the data lead me to believe that there was another process that caused the volcanic sediments to eventually settle in different areas than what was predicted. Processes such as weathering and currents could have moved around the sediments over the last hundred years. Other processes have likely moved the sediments and mixed the sediments from the 1866 eruption with the volcanic sediments from the eruptions to the east.

Conclusion

Through this research, I was looking to complete the missing bathymetric mapping between the Manu'a islands in American Samoa, especially mapping the caldera from the 1866 volcanic eruption. In combination with the mapping, I wanted to see if the volcanic sediments settled in a gradient and if I could correlate backscatter values to grain size values.

While completing the mapping of the caldera we found a series of calderas on the ridge, east of the 1866 eruption. This means there are multiple sets of plumbing, and the volcanic sediments on the seabed are from multiple eruptions over at least the last 200 years. Based on the eight grab samples, the volcanic sediment was poorly sorted and was characterized as fine sand to coarse gravel.

There was a weak trend between grain size and distance from the caldera, with the sediments close to the caldera generally being larger and having faster-settling velocities. The backscatter values had no correlation to grain size and no significant trends. Angularity showed the two predominant outlier points, locations Am Sam 5 and 7, were both sub-rounded and highly spherical compared to the rest of the samples. This indicates that they went through other processes that affected their physical appearance and where they settled. The series of calderas on the ridge, in accordance with evidence of multiple large landslides, are possible factors in why the grain size and backscatter data have little correlation.

Future research is needed in the field of seafloor mapping and marine volcanic eruptions because understanding the seafloor is pivotal, as it holds many mysteries about the start of life on Earth and plays a pivotal role in biological, chemical, and physical processes.

Acknowledgements

I would like to sincerely thank the School of Oceanography at the University of Washington for making this research experience possible. I would like to thank my advisor Professor Ogston, and the graduate students in her lab for their support. I would like to thank the crew and captain of the R/V Thomas G. Thompson, who made this data collection possible. Lastly, I would like to thank the other students in the senior class, especially the MG&G group and Jenna Fernandez, my parents, and Emma Robins for their endless support.

References

Barber, R., McCoy, B., & Ramirez, R. (2023). Why mapping the entire seafloor is a daunting task, but key to improving human life. NPR. https://www.npr.org/transcripts/1198908501

Beccario, C. (2024). A global map of wind, weather, and ocean conditions. Earth. nullschool.net

Blott, S. (2020). Version 9.1 GRADISTAT. Kenneth Pye Associates Ltd.

Cañón-Tapia, E., & Walker, G. P. L. (2004). Global aspects of volcanism: The perspectives of "Plate tectonics" and "volcanic systems." Earth-Science Reviews, 66(1–2), 163–182. doi.org/10.1016/j.earscirev.2003.11.001

Cassidy, M., Watt, S., Palmer, M., Trofimovs, J., Symons, W., Maclachlan, S., & Sinton, A. (2014). Construction of volcanic records from marine sediment cores: A review and Case Study (montserrat, West Indies). Earth-Science Reviews. University of Birmingham. https://research.birmingham.ac.uk/en/publications/construction-of-volcanic-records-from-marine-sediment-cores-a-rev

Gardner, J. V., B. R. Calder, and A. A. Armstrong. (2021). Geomorphometric descriptions of archipelagic aprons off the southern flanks of French Frigate Shoals and Necker Island Edifices, Northwest Hawaiian ridge, GSA Bulletin, 133(9–10), 2189–2209, doi:10.1130/b35875.1.

Hawaiian Volcano Observatory. (2022). Reference map of the volcanic islands of American samoa, Reference map of the volcanic islands of American Samoa | U.S. Geological

Survey. Available from: https://www.usgs.gov/media/images/reference-map-volcanic-islands-american-samoa (Accessed 30 October 2023)

Hellequin, L., Boucher, J-M, and Lurton, X. (2003). "Processing of high-frequency multibeam echo sounder data for seafloor characterization," in IEEE Journal of Oceanic Engineering, vol. 28, no. 1, pp 78-89. doi: 10.1109/JOE.2002.808205.

Houghton, B., J. White, and A. Van Eaton. (2015). Phreatomagmatic and related eruption styles, The Encyclopedia of Volcanoes (Second Edition). Houghton, B., J. White, and A. Van Eaton (2015), Phreatomagmatic and related eruption styles, The Encyclopedia of Volcanoes (Second Edition). doi.org/10.1016/B978-0-12-385938-9.00030-4

Jackson, M. (2017). American samoa expedition: Suesuega o le Moana O Amerika samoa, Background: Volcanic Islands and Seamounts in the Samoan Region: NOAA Office of Ocean Exploration and Research. https://oceanexplorer.noaa.gov/okeanos/explorations/ex1702/background/plan/welcome.html

Levitan, Z. (2024). Morphology of Submarine Landslides on the Flanks of the Manu'a islands, American Samoa, University of Washington.

Maeno, F., Kaneko, T., Ichihara, M., Suzuki, Y. J., Yasuda, A., Nishida, K., & Ohminato, T. (2022). Seawater-magma interactions sustained the high column during the 2021 phreatomagmatic eruption of Fukutoku-Oka-no-ba. Nature News. https://api.semanticscholar.org/CorpusID:253240690

Morgan, J. K., and D. A. Clague. (2003). Volcanic spreading on Mauna Loa Volcano, Hawaii: Evidence from accretion, alteration, and exhumation of volcaniclastic sediments, Geology. doi.org/10.1130/0091-7613(2003)031<0411:VSOMLV>2.0.CO;2

Morgan, J. K., G. F. Moore, D. J. Hills, and S. Leslie. (2000). Overthrusting and sediment accretion along Kilauea's Mobile South Flank, Hawaii: Evidence for volcanic spreading from marine seismic reflection data, Geology. doi.org/10.1130/0091-7613(2000)28<667:OASAAK>2.0.CO;2

Rehm, E., and P. Halbach. (2003). Hawaiian-derived volcanic ash layers in equatorial northeastern Pacific sediments, Marine Geology. doi.org/10.1016/0025-3227(82)90059-7

Rubin, K. H., Soule, S.A., Chadwick, W. W., Fornari, D. J., Clague, D. A., Embley, R. W., Baker, E. T., Perfit, M. R., Caress, D. W., & Dziak, R. P. (2012). Volcanic Eruptions in the Deep Sea. *Oceanography, 25(1), 142–157.* http://www.jstor.org/stable/24861152

Ryan, W. B. F., Carbotte, S. M., Coplan, J. O., O'Hara, S., Melkonian, A., Arko, R., Weissel, R. A., Ferrini, V., Goodwillie, A., Nitsche, F., Bonczkowski, J.,
and Zemsky, R. (2009). Global Multi-Resolution Topography synthesis. Geochemistry, Geophysics, Geosystems, 10, Q03014, doi:10.1029/2008GC002332.

Pettijohn, F. J., & Krumbein, W. C. (1988). Manual of Sedimentary Petrography. Appleton Century Crofts Inc.

Wattson, S., J. Whittaker, V. Lucieer, M. Coffin, and G. Lamarche. (2017). Erosional and depositional processes on the submarine flanks of Ontong Java and Nukumanu Atolls, Western Equatorial Pacific Ocean, Marine Geology. doi.org/10.1016/j.margeo.2017.08.006

USGS, Why is it important to monitor volcanoes? U.S. Geological Survey. Why is it important to monitor volcanoes? | U.S. Geological Survey (usgs.gov)